# *Supporting Information*

## Azide-Coordination in Homometallic Dinuclear Lanthanide(III) Complexes Containing Non-Equivalent Lanthanide Metal Ions: Zero Field SMM Behavior in the Dysprosium Analogue

*Pawan Kumar,[a] Sourav Biswas,[b] Abinash Swain,[c] Joydev Acharya,[a] Vierandra Kumar,[a] Pankaj Kalita,[d] Jessica Flores Gonzalez,[e] Olivier Cador,[e] Fabrice Pointillart,*[e] Gopalan Rajaraman*[c] and Vadapalli Chandrasekhar*[a,d]*

[a]Department of Chemistry, Indian Institute of Technology Kanpur, Kanpur-208016, India

[b]Department of Geo-Chemistry, Keshav Deva Malaviya Institute of Petroleum Exploration, Dehradun-248915, India.

[c]Department of Chemistry, Indian Institute of Technology Bombay, Powai, Mumbai 400076.

[d]Tata Institute of Fundamental Research, Gopanpally, Hyderabad - 500 107, India,

[e]Institut des Sciences Chimiques de Rennes, UMR 6226 CNRS-Université de Rennes 1, 263 Avenue du Genéral Leclerc, 35042, Rennes Cedex, France

AUTHOR EMAIL ADDRESS: vc@iitk.ac.in; vc@tifrh.res.in; fabrice.pointillart@univ-rennes1.fr; rajaraman@chem.iitb.ac.in

**Table S1**. Crystal data and structure refinement parameters of **3**

| | **3** |
|---|---|
| formula | $C_{37}H_{43}Gd_2N_{11}O_9$ |
| g/mol | 1100.32 |
| crystal system | Monoclinic |
| space group | $P\text{-}2_1/c$ |
| $a$/Å | 14.519(5) |
| $b$/Å | 21.287(7) |
| $c$/Å | 15.950(6) |
| $\alpha$ (°) | 90 |
| $\beta$(°) | 116.227(10) |
| $\gamma$(°) | 90 |
| $V$/Å$^3$ | 4422.4(3) |
| $Z$ | 4 |
| $\rho_c$/g cm$^{-3}$ | 1.653 |
| $\mu$/mm$^{-1}$ | 3.035 |
| $F$(000) | 2168.0 |
| cryst size (mm$^3$) | 0.19 × 0.17 × 0.15 |
| $2\theta$ range (deg) | 5.93 to 56.62 |
| limiting indices | -19<=h<=19<br>-28<=k<=28<br>-21<=l<=21 |
| reflns collected | 69233 |
| ind reflns | 10983 [R(int) =0.0447] |
| Completeness to $\theta$ (%) | 100 |
| refinement method | Full-matrix least-squares on $F^2$ |
| data/restraints/params | 10983/12/539 |
| goodness-of-fit on $F^2$ | 1.045 |
| Final R indices<br>[$I > 2\theta(I)$] | $R_1$ = 0.0269<br>$wR_2$ = 0.0661 |
| $R$ indices (all data) | $R_1$ = 0.0341<br>$wR_2$ = 0.0696 |
| CCDC no. | 2026242 |

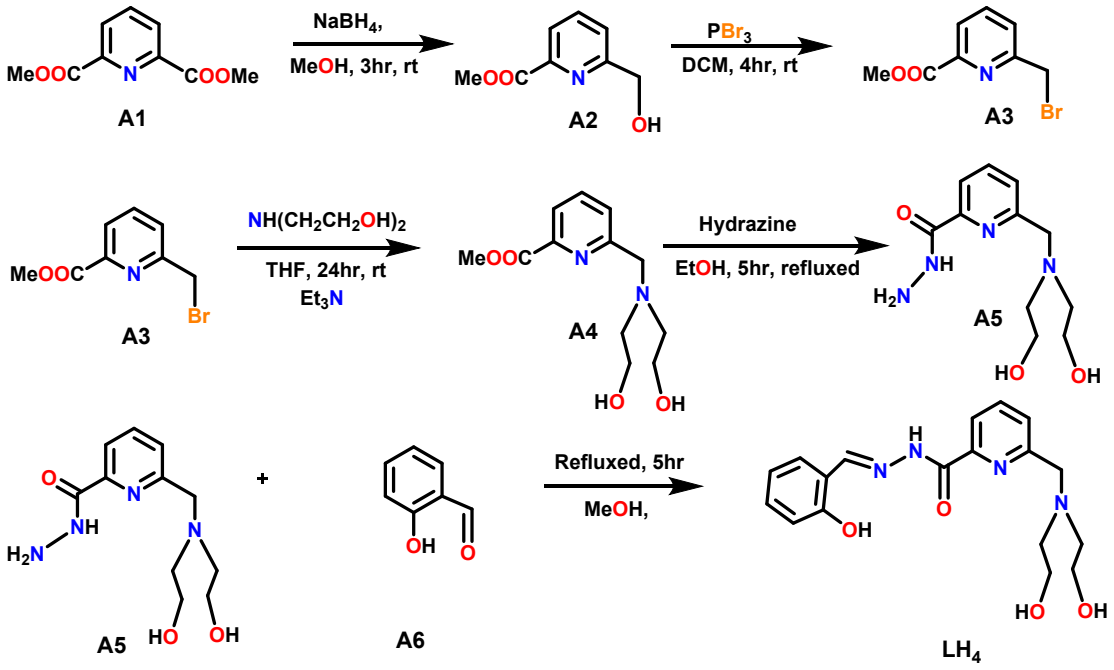


**Scheme S1.** Synthesis of $LH_4$.

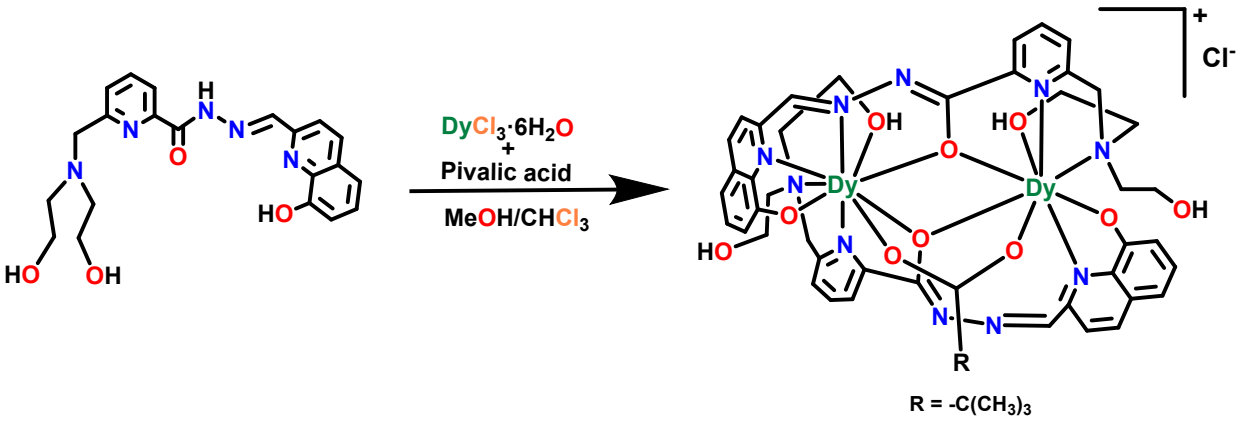


**Scheme S2.** Synthesis of a dinuclear complex, $[Dy_2(LH_2)_2(\mu_2\text{-}\eta^1\text{:}\eta^1\text{-Piv})]Cl{\cdot}2MeOH{\cdot}2H_2O$[11d]

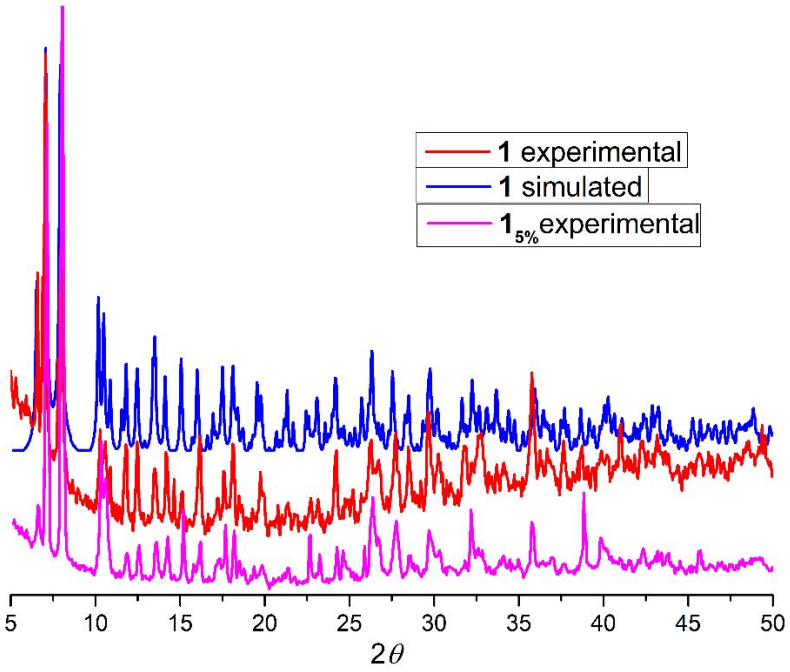


**Figure S1.** Experimental XRD pattern and simulated XRD from single crystal data for **1** along with experimental pattern of $\mathbf{1}_{5\%}$.

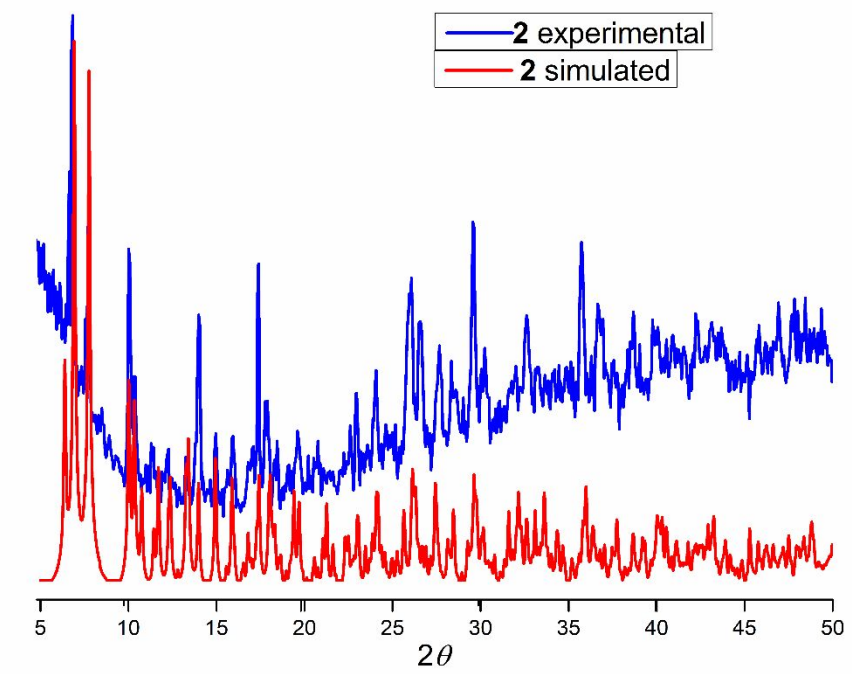


**Figure S2.** Experimental XRD pattern and simulated XRD from single crystal data for **2**.

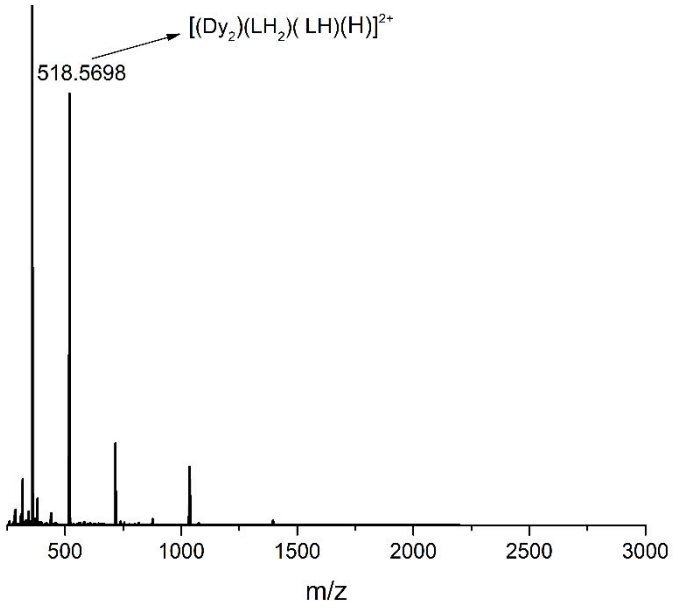
[(Dy2)(LH2)( LH)(H)]2+
518.5698
500
1000
1500
2000
2500
3000
m/z

(a)

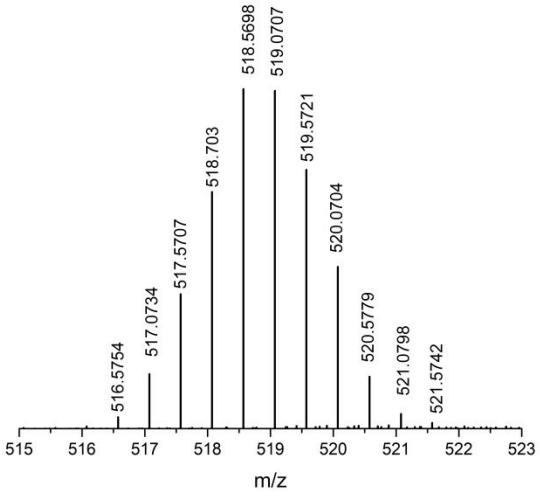
516.5754
517.0734
517.5707
518.703
518.5698
519.0707
519.5721
520.0704
520.5779
521.0798
521.5742
515
516
517
518
519
520
521
522
523
m/z

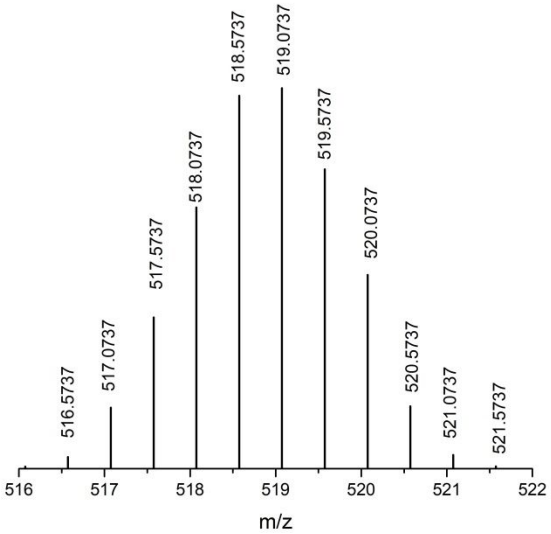
516.5737
517.0737
517.5737
518.0737
518.5737
519.0737
519.5737
520.0737
520.5737
521.0737
521.5737
516
517
518
519
520
521
522
m/z

(b) (c)

**Figure S3**. **a)** Full range ESI-MS spectrum of complex **1**. **b)** Experimental and **c)** simulated isotopic distribution pattern of the fragment $[Dy_2(LH_2)(LH)H]^{2+}$.

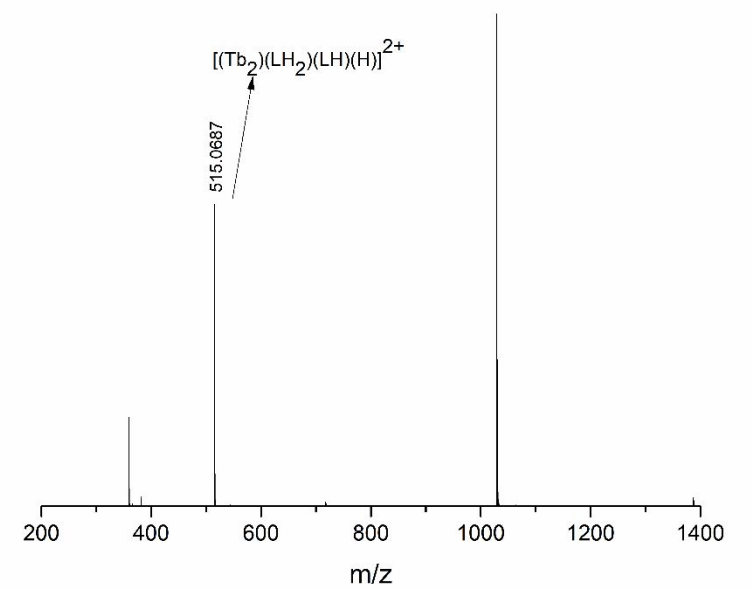


**(a)**

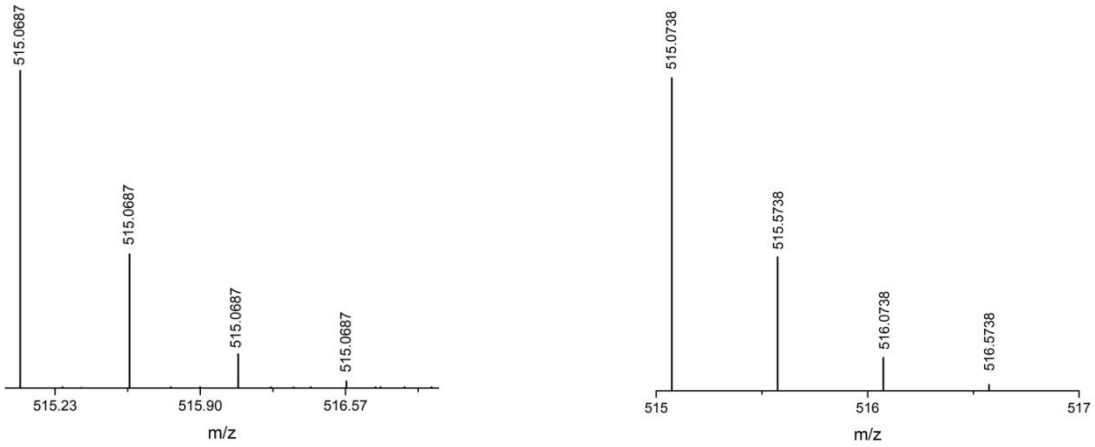


**(b)** **(c)**

**Figure S4. a)** ESI-MS spectrum of complex **2**. **b)** Experimental and **c)** simulated mass spectral pattern of the fragment $[Tb_2(LH_2)(LH)H]^{2+}$ .

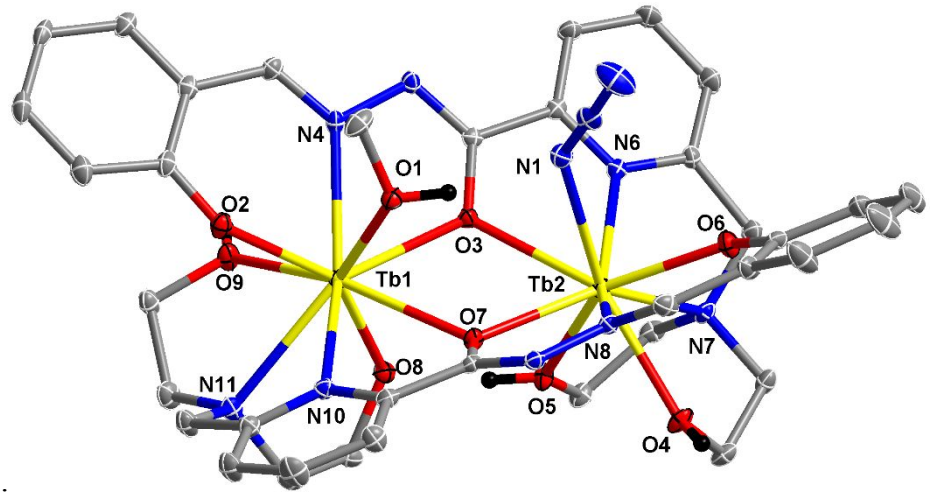


**Figure S5**. Molecular Structure of compound **2** as thermal ellipsoids at 50% probability level (selected hydrogen atoms and the solvent molecules have been omitted for clarity). Colour codes: N = blue; O = red; C = grey; Tb = yellow and H = black

**Table S2**. Selected Bond Distances (Å) and Bond angles (°) for compound **2**

| Bond distances around Tb1 | | Bond distances around Tb2 | | Bond angles around Tb | |
|---|---|---|---|---|---|
| Tb(1)-O(7) | 2.590(17) | Tb(2)-O(7) | 2.356(17) | Tb(1)-O(3)-Tb(2) | 115.57(7) |
| Tb(1)-O(8) | 2.334(18) | Tb(2)-O(3) | 2.507(17) | Tb(1)-O(7)-Tb(2) | 114.48(7) |
| Tb(1)-O(3) | 2.369(18) | Tb(2)-O(5) | 2.391(18) | | |
| Tb(1)-O(9) | 2.537(18) | Tb(2)-O(4) | 2.425(18) | | |
| Tb(1)-O(2) | 2.247(18) | Tb(2)-O(6) | 2.232(18) | | |
| Tb(1)-O(1) | 2.503(18) | Tb(2)-N(6) | 2.503(2) | | |
| Tb(1)-N(11) | 2.641(2) | Tb(2)-N(8) | 2.522(2) | | |
| Tb(1)-N(10) | 2.536(2) | Tb(2)-N(7) | 2.646(2) | | |
| Tb(1)-N(4) | 2.519(2) | Tb(2)-N(1) | 2.571(2) | | |

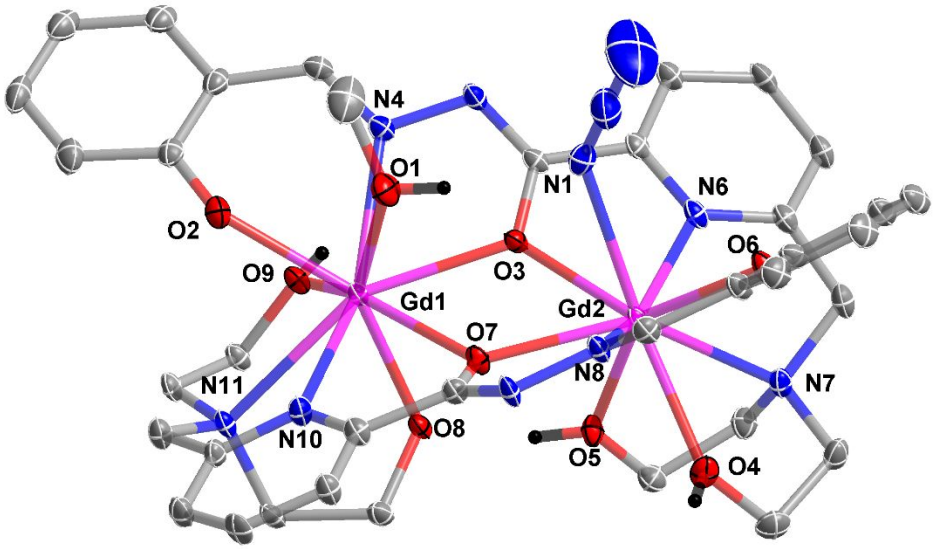


**Figure S6**. Molecular Structure of compound **3** as thermal ellipsoids at 50% probability level (selected hydrogen atoms and the solvent molecules have been omitted for clarity). Colour codes: N = blue; O = red; C = grey; Gd = pink and H = black

**Table S3**. Selected Bond Distances (Å) and Bond angles (°) for compound **3**

| Bond distances around Gd1 | | Bond distances around Gd2 | | Bond angles around Gd | |
|---|---|---|---|---|---|
| Gd(1)-O(7) | 2.526(2) | Gd(2)-O(7) | 2.376(2) | Gd(1)-O(3)-Gd(2) | 116.11(8) |
| Gd(1)-O(8) | 2.383(2) | Gd(2)-O(3) | 2.494(2) | Gd(1)-O(7)-Gd(2) | 114.62(8) |
| Gd(1)-O(3) | 2.367(2) | Gd(2)-O(5) | 2.391(2) | | |
| Gd(1)-O(9) | 2.531(2) | Gd(2)-O(4) | 2.471(2) | | |
| Gd(1)-O(2) | 2.293(2) | Gd(2)-O(6) | 2.268(2) | | |
| Gd(1)-O(1) | 2.489(2) | Gd(2)-N(6) | 2.537(2) | | |
| Gd(1)-N(11) | 2.669(2) | Gd(2)-N(8) | 2.515(3) | | |
| Gd(1)-N(10) | 2.625(3) | Gd(2)-N(7) | 2.671(3) | | |
| Gd(1)-N(4) | 2.553(3) | Gd(2)-N(1) | 2.552(3) | | |

**Table S4.** Continuous Shape Measures (CShM) calculations for $Ln^{III}$

| Complex | Structure† | | | | |
|---|---|---|---|---|---|
| | JCSAPR-9 | CSAPR-9 | JTCTPR-9 | TCTPR-9 | **MFF-9** |
| **1**_Dy1 CShM | 3.039 | 2.261 | 3.663 | 3.040 | **1.432** |
| **1**_Dy2 CShM | 2.093 | 1.264 | 2.139 | 2.102 | **0.905** |
| **2**_Tb1 CShM | 3.033 | 2.244 | 3.672 | 3.040 | **1.415** |
| **2**_Tb2 CShM | 2.169 | 1.304 | 2.248 | 2.168 | **0.908** |
| **3**_Gd1 CShM | 3.055 | 2.300 | 2.970 | 3.239 | **1.619** |
| **3**_Gd2 CShM | 2.741 | 1.778 | 2.497 | 2.403 | **1.159** |

† *JCSAPR-9 = Capped square antiprism J10 (C4v); CSAPR-9 = Spherical capped square antiprism (C4v); JTCTPR-9 = Tricapped trigonal prism J51 (D3h); TCTPR-9 = Spherical tricapped trigonal prism (D3h); MFF-9 = Muffin (Cs)*

The crystal packing analysis of **1** reveals the presence of intramolecular as well as intermolecular hydrogen bonding interactions. Two sets of intramolecular hydrogen bonding are encountered in **1**: in one set, two strong hydrogen bonding are formed between the –$CH_2CH_2OH$ of a $[LH_2]^{2-}$ and the O of the deprotonated arm of $[LH]^{3-}$ with D–H…..A, 1.814 Å while in other set is between methanol (OH) and azide ion (-N1····H1-O1) with D-H….A, 2.038 Å (Figure S7).

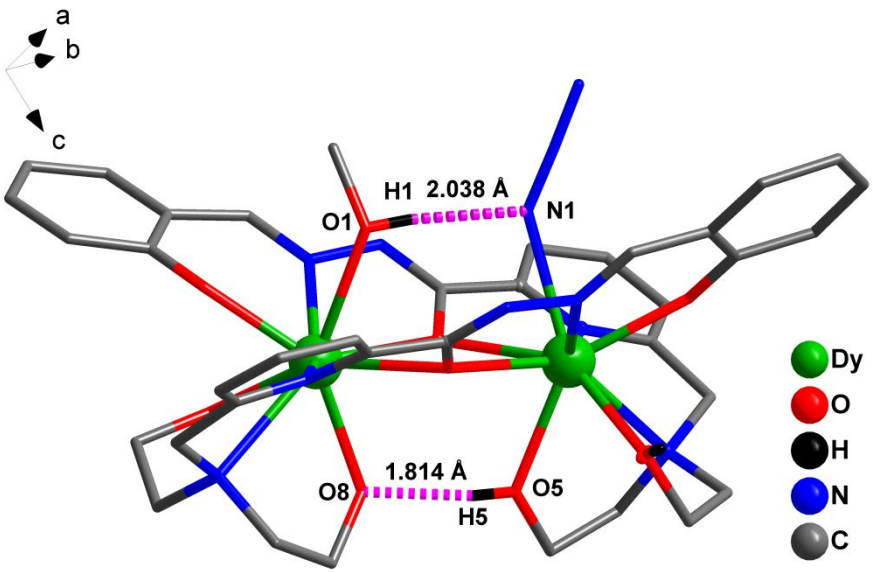

**Figure S7:** Two set of intramolecular hydrogen bonding of complex **1** (selected hydrogen atoms have been omitted for clarity).

An analysis of the crystal packing **1** reveals that it is possible to hierarchically construct its supramolecular structure. First a 1D chain is generated as a result of a pair of intermolecular hydrogen bonding in two set: in one set each complex is connected to other via a pair of hydrogen bonding between O–H of a diethanolammine arm (–$CH_2CH_2OH$) to another –O of deprotonated diethanolamine arm (-CH2CH2O-) with D-H….A, 2.008 Å and second set each complex is connected to other via a pair of hydrogen bonding between the OH of diethanol amine arm of $[LH_2]^{2-}$ and imine nitrogen of $[LH]^{3-}$ (O4-H4···N9) with D-H..A, 2.059 Å (Figure S8). Bond parameters involved in this hydrogen bonding are given in Table S5.

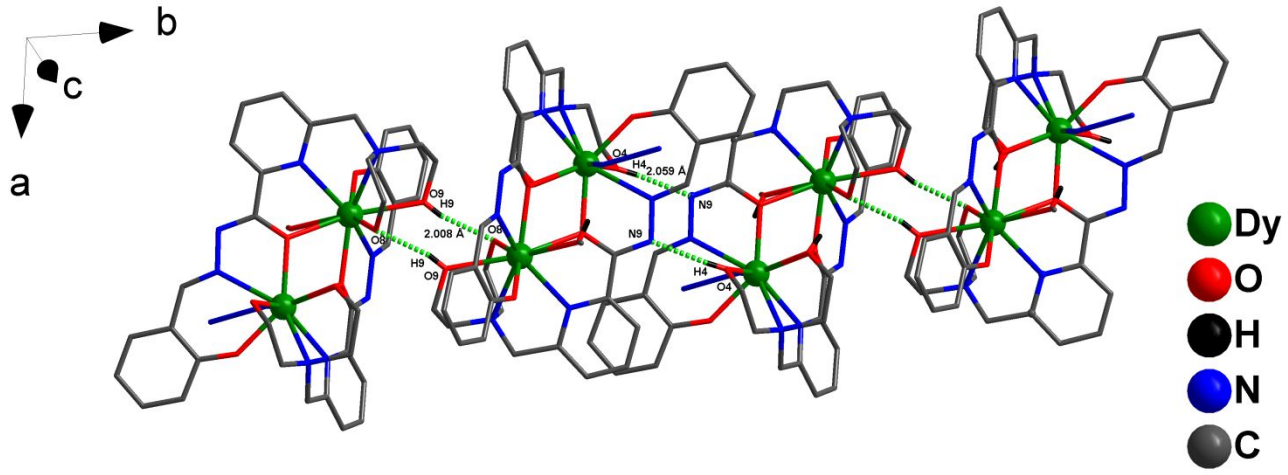


**Figure S8.** 1D supramolecular structure of complex **1** (selected carbon, hydrogen are omitted for clarity)

**Table S5**: Hydrogen bond parameter for complex **1**.

| D-H---A | H---A | D---A | D-H---A |
|---|---|---|---|

| | | | |
|---|---|---|---|
| (intra)O5-H5---O8 | 1.8138(333) | 2.5025(26) | 171.364(3792) |
| (intra)O1-H1---N1 | 2.0384(328) | 2.7904(29) | 171.219(3400) |
| (inter)O9-H9---O8 | 2.0076(329) | 2.7222(25) | 166.722(3510) |
| (inter)O4-H4---N9 | 2.0593(334) | 2.7429(28) | 175.684(3708) |

Table S4.

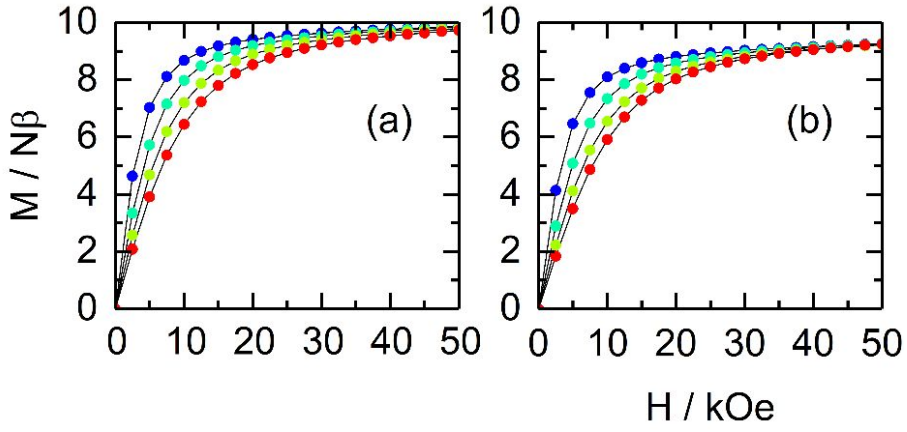


**Figure S9**. Field dependence of the magnetization from 2 to 5 K for **1** (a) and **2** (b).

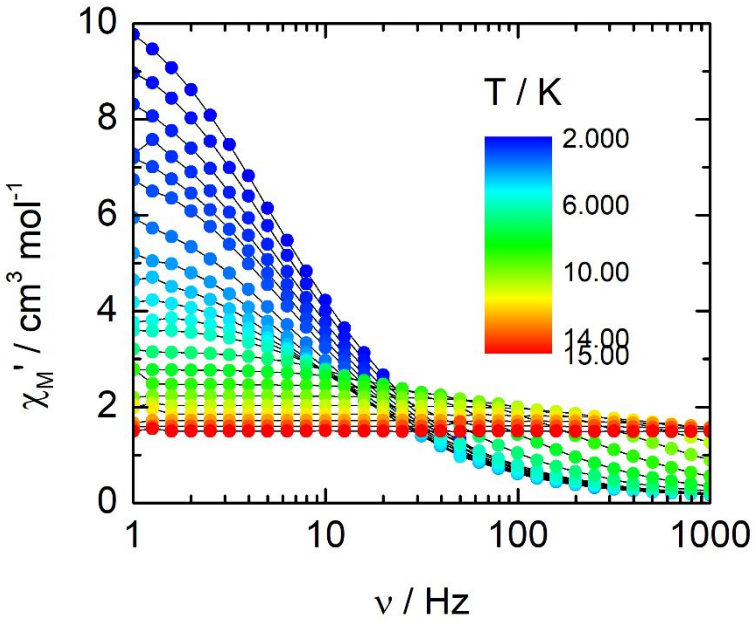


**Figure S10**. In-phase component of the ac magnetic susceptibility data for **1**, from 2 to 15 K under 0 Oe.

**Extended Debye:**

$$\chi_M' = \chi_S + (\chi_T - \chi_S)\frac{1+(\omega\tau)^{1-\alpha}\sin\left(\alpha\frac{\pi}{2}\right)}{1+2(\omega\tau)^{1-\alpha}\sin\left(\alpha\frac{\pi}{2}\right)+(\omega\tau)^{2-2\alpha}}$$

$$\chi_M'' = (\chi_T - \chi_S)\frac{(\omega\tau)^{1-\alpha}\cos\left(\alpha\frac{\pi}{2}\right)}{1+2(\omega\tau)^{1-\alpha}\sin\left(\alpha\frac{\pi}{2}\right)+(\omega\tau)^{2-2\alpha}}$$

With $\chi_T$ the isothermal susceptibility, $\chi_S$ the adiabatic susceptibility, $\tau$ the relaxation time and $\alpha$ an empiric parameter which describe the distribution of the relaxation time. For SMM with only one relaxing object $\alpha$ is close to zero. The extended Debye model was applied to fit simultaneously the experimental variations of $\chi_M$' and $\chi_M$'' with the frequency $\nu$ of the oscillating field ($\omega = 2\pi\nu$). Typically, only the temperatures for which a maximum on the $\chi_M$''

*vs.* $\nu$ curves, have been considered (see figure here below for an example). The best fitted parameters $\tau$, $\alpha$, $\chi_T$, $\chi_S$ are listed in Tables S5 to S7 with the coefficient of determination $R^2$.

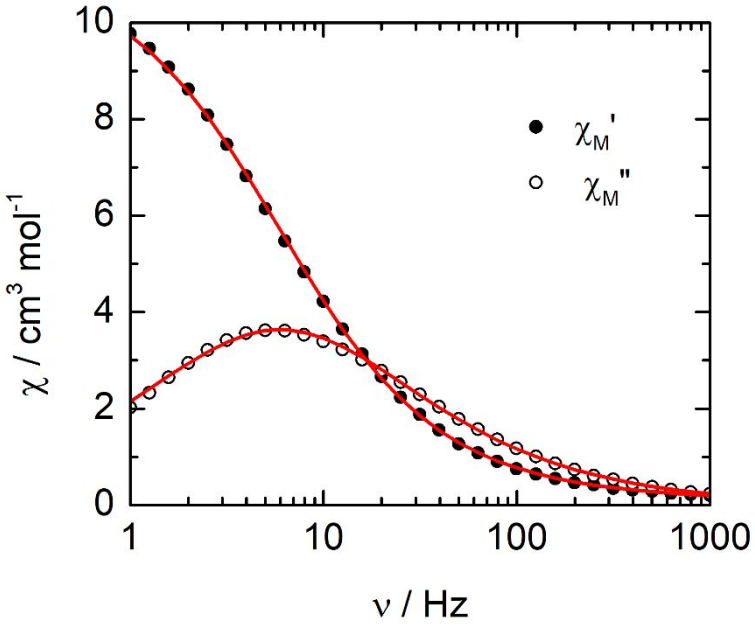


**Figure S11.** Frequency dependence of the in-phase ($\chi_M$') and out-of-phase ($\chi_M$") components of the *ac* susceptibility measured on powder at 2 K and 0 Oe with the best fitted curves (red lines) for **1**.

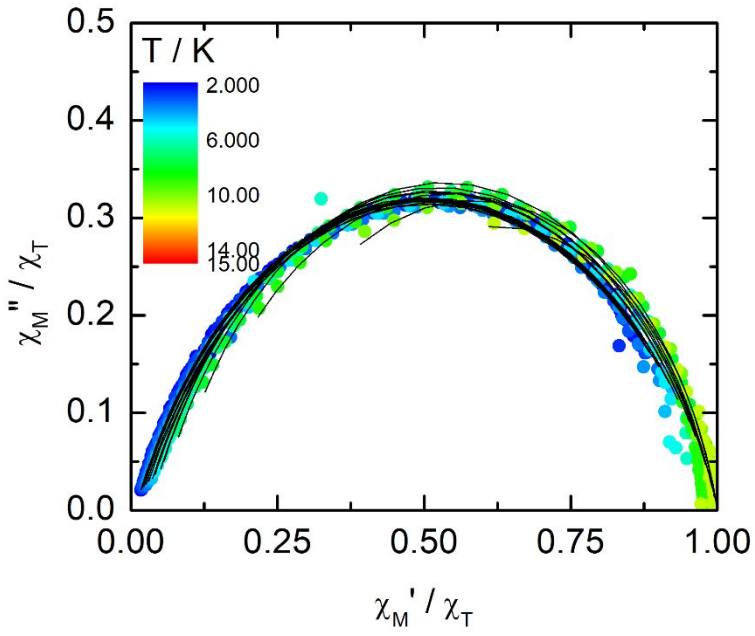

**Figure S12**. Normalized Cole-Cole plot at several temperatures between 2 and 15 K for **1**.

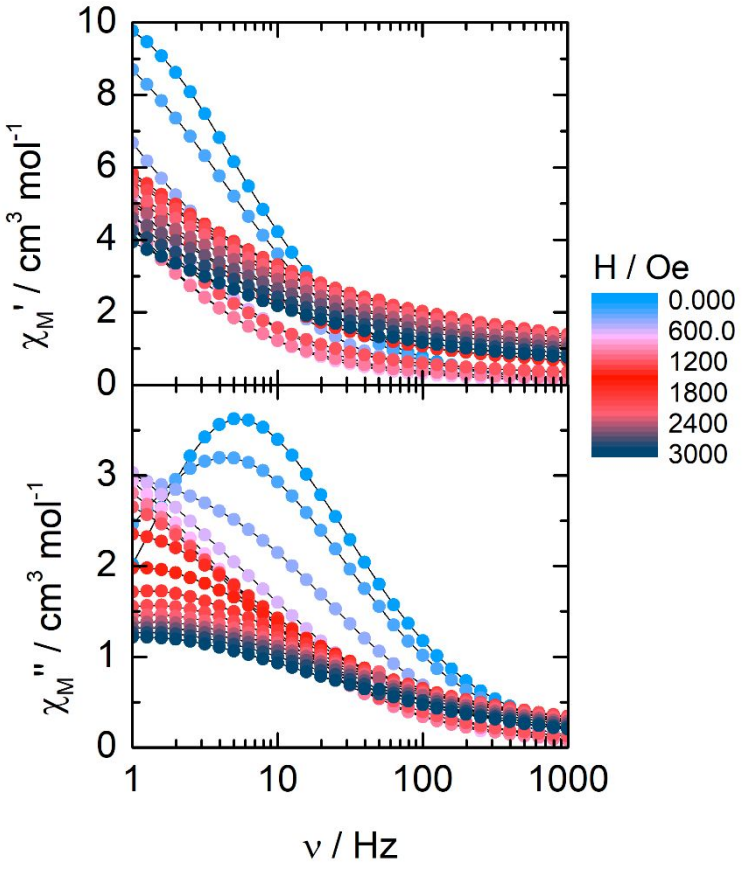


**Figure S13**. In-phase and out-of-phase components of the *ac* magnetic susceptibility for **1** at 2 K in an applied *dc* magnetic field from 0 to 3000 Oe.

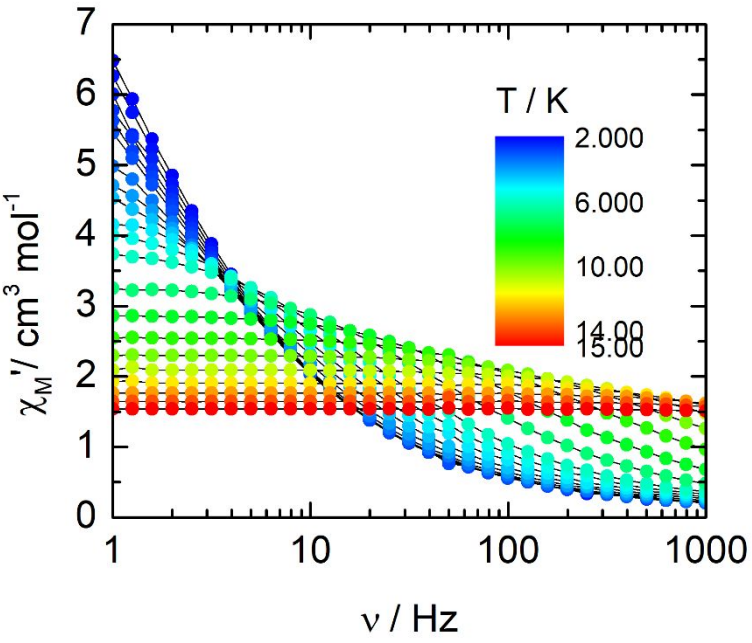


**Figure S14**. In-phase component of the *ac* magnetic susceptibility data for **1**, from 2 to 15 K under 800 Oe.

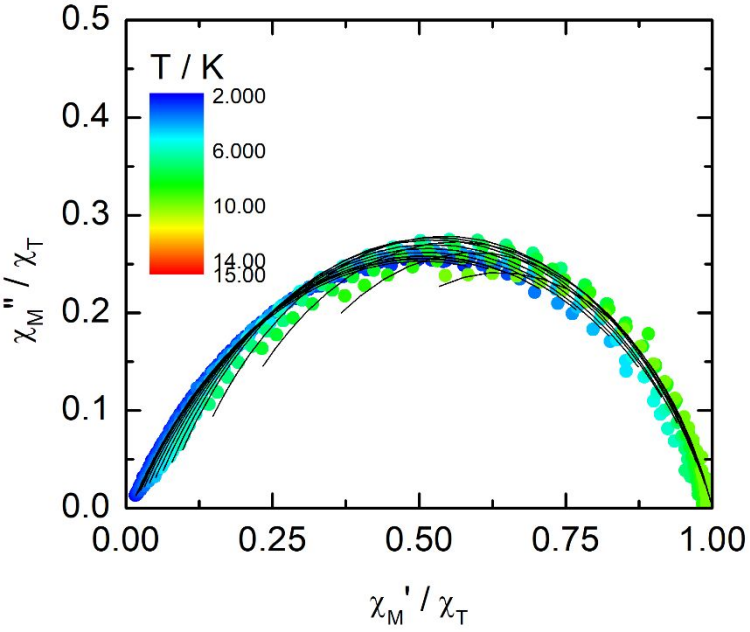


**Figure S15**. Normalized Cole-Cole plot at several temperatures between 2 and 15 K for **1** under 800 Oe.

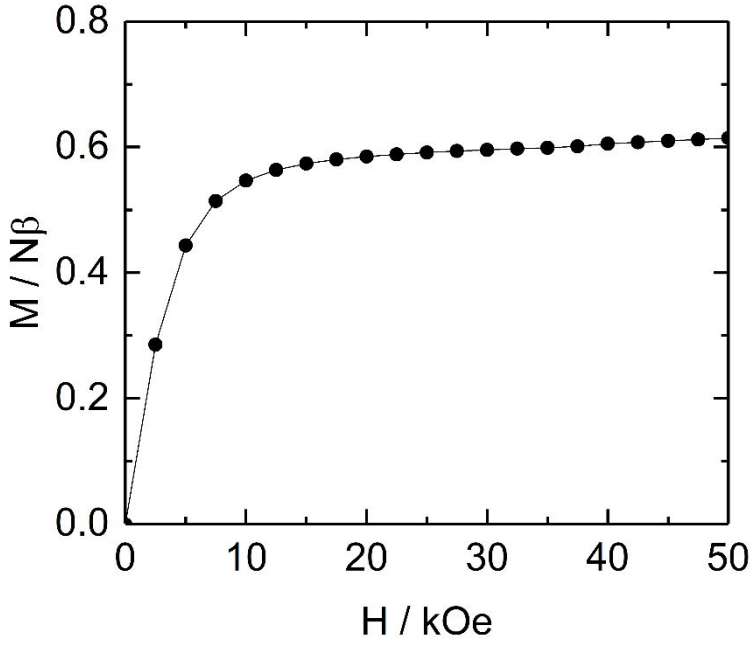


**Figure S16**. Field dependence of the magnetization for $\mathbf{1}_{5\%}$ at 2 K.

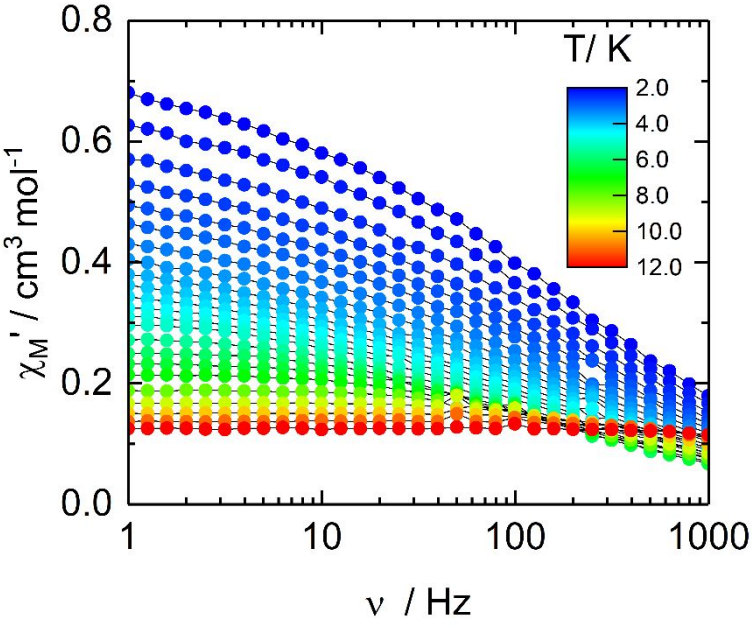


**Figure S17**. In-phase component of the *ac* magnetic susceptibility data for $\mathbf{1}_{5\%}$, from 2 to 15 K under 0 Oe.

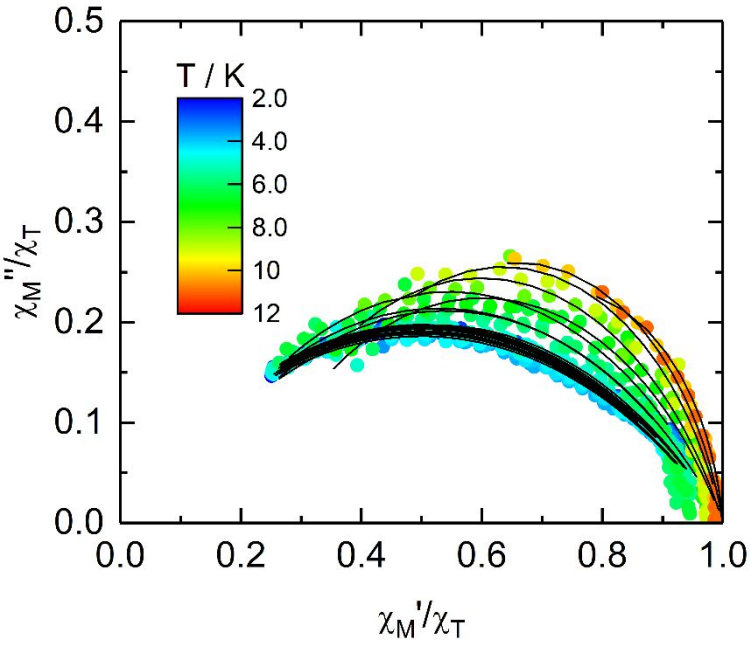


**Figure S18**. Normalized Cole-Cole plot at several temperatures between 2 and 11 K for $\mathbf{1}_{5\%}$ under zero magnetic field.

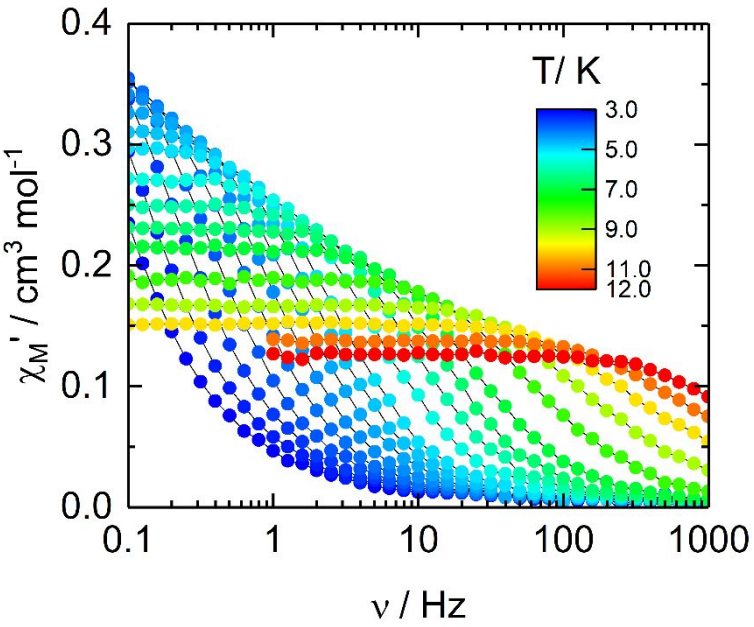


**Figure S19**. In-phase component of the *ac* magnetic susceptibility data for $\mathbf{1}_{5\%}$, from 2 to 11 K under 800 Oe..

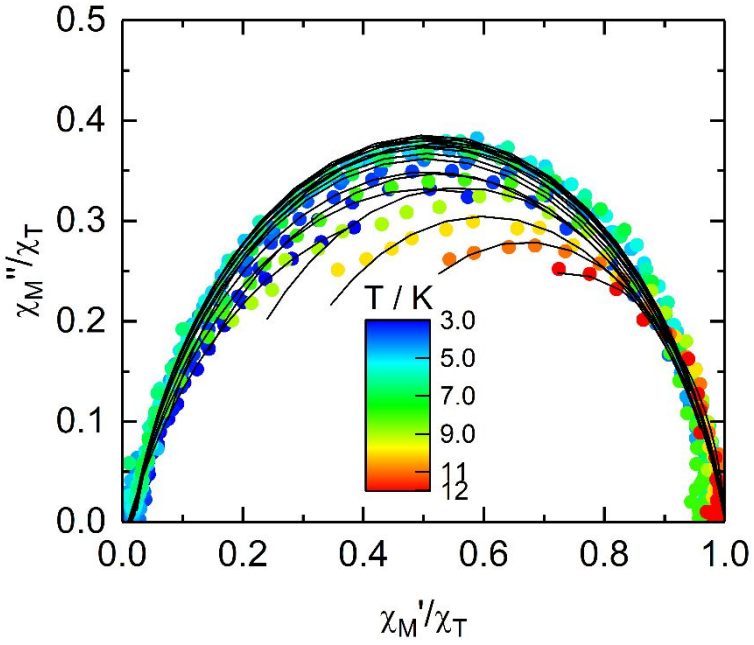


**Figure S20**. Normalized Cole-Cole plot at several temperatures between 3 and 12 K for $\mathbf{1}_{5\%}$ under 800Oe.

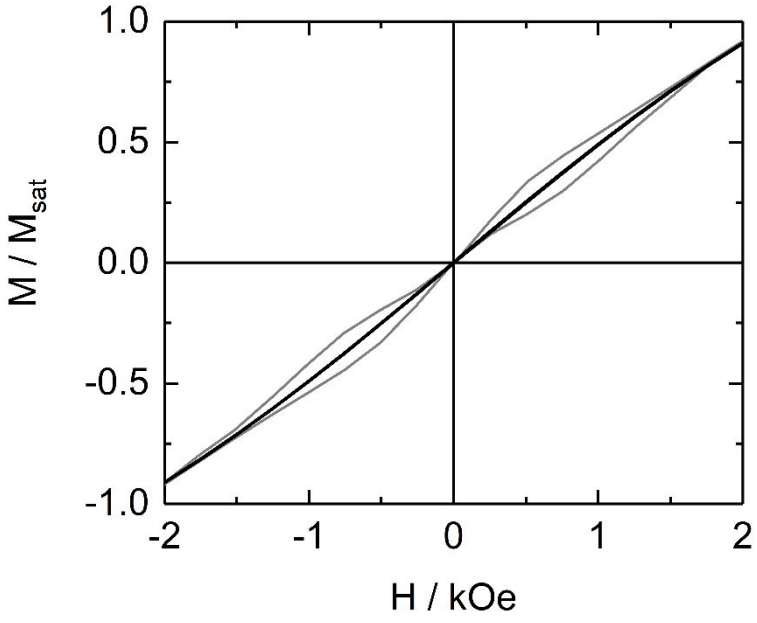

**Figure S21**. Normalized hysteresis loops of the magnetization for **1** (black lines) and $\mathbf{1}_{5\%}$ (grey lines) at 2 K.

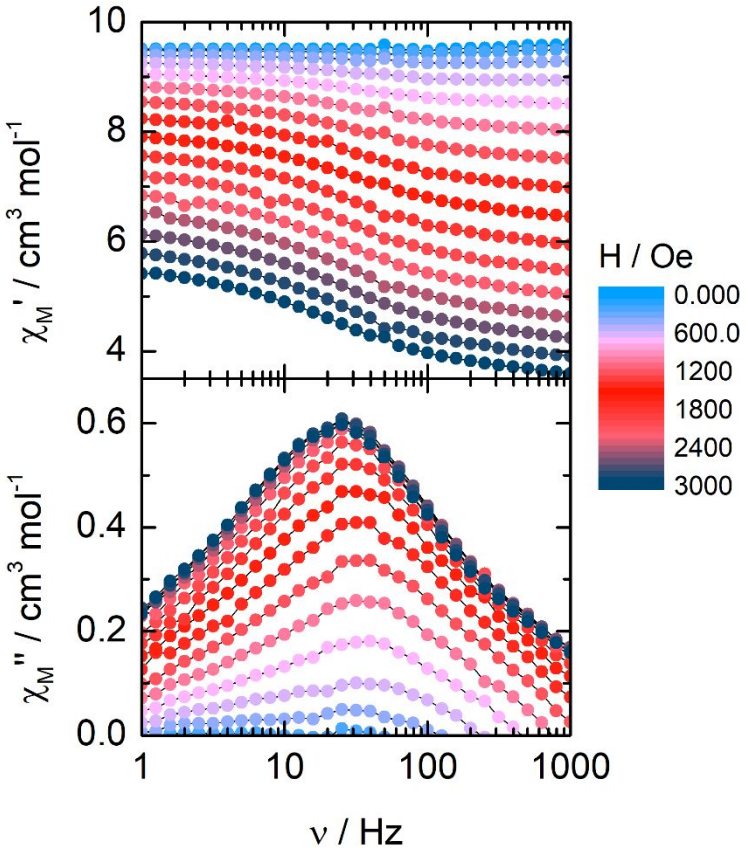


**Figure S22**. In-phase and out-of-phase components of the *ac* magnetic susceptibility for **2** at 2 K in an applied *dc* magnetic field from 0 to 3000 Oe.

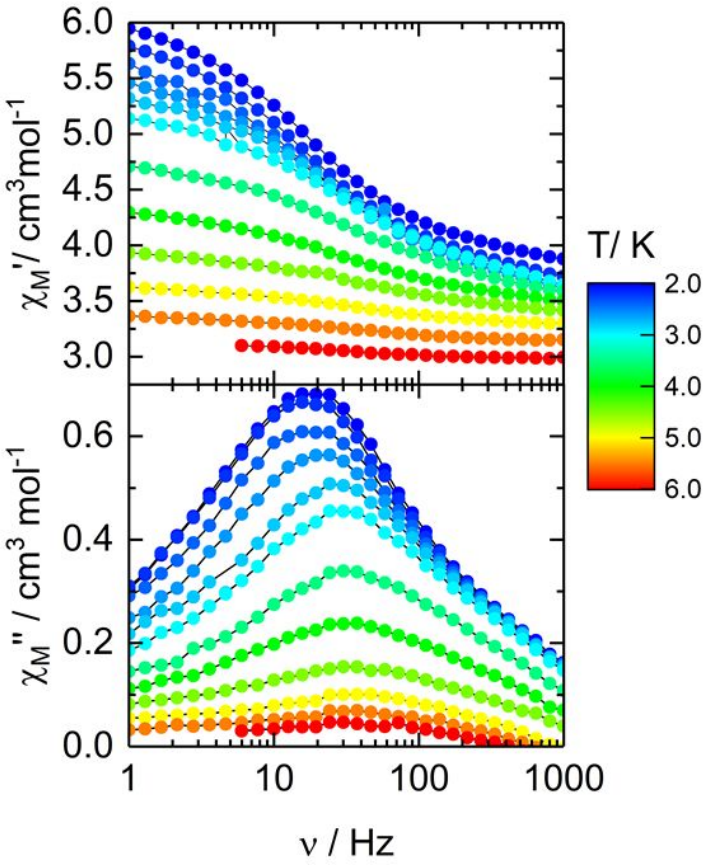


**Figure S23**. In-phase ($\chi_M$') and Out-of-phase ($\chi_M$'') components of the *ac* magnetic susceptibility data for **2** in 2800 Oe applied magnetic field in the temperature range of 2-6 K.

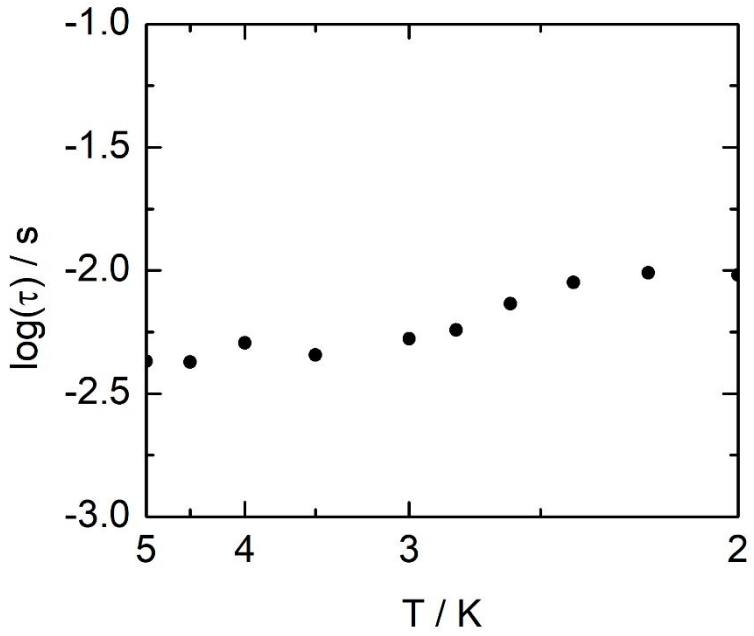


**Figure S24**. Thermal dependence of the magnetic relaxation time for **2** in 2800 Oe applied magnetic field (full black circles) in the 2-5 K temperature range.

**Table S6**. Best fitted parameters ($\chi_T$, $\chi_S$, $\tau$ and $\alpha$) with the extended Debye model for compound **1** at 0 Oe in the temperature range 2-11 K.

| T / K | $\chi_S$ / $cm^3mol^{-1}$ | $\chi_T$ / $cm^3mol^{-1}$ | $\tau$ / s | $\alpha$ | $R^2$ |
|---|---|---|---|---|---|
| 2 | 0.08762 | 11.33742 | 0.02675 | 0.26889 | 0.99979 |
| 2.2 | 0.0771 | 10.46142 | 0.02568 | 0.2722 | 0.9998 |
| 2.4 | 0.0817 | 9.56701 | 0.02462 | 0.27313 | 0.99975 |
| 2.6 | 0.07762 | 8.73469 | 0.02319 | 0.27026 | 0.99912 |
| 2.8 | 0.07511 | 8.20648 | 0.02270 | 0.2736 | 0.99979 |
| 3 | 0.07909 | 7.66048 | 0.02187 | 0.27483 | 0.99982 |
| 3.5 | 0.08531 | 6.61609 | 0.01972 | 0.27867 | 0.99961 |
| 4 | 0.09105 | 5.76750 | 0.01706 | 0.27509 | 0.99964 |
| 4.5 | 0.10856 | 5.09633 | 0.01410 | 0.26637 | 0.9993 |
| 5 | 0.10791 | 4.58915 | 0.01151 | 0.26343 | 0.99949 |
| 5.5 | 0.13001 | 4.09939 | 0.00868 | 0.24505 | 0.99872 |
| 6 | 0.12605 | 3.79210 | 0.00669 | 0.24169 | 0.99942 |

| | | | | | |
|---|---|---|---|---|---|
| 7 | 0.14926 | 3.25215 | 0.00359 | 0.22709 | 0.99960 |
| 8 | 0.18730 | 2.82320 | 0.00169 | 0.20551 | 0.99970 |
| 9 | 0.21791 | 2.53317 | 7.55E-04 | 0.21268 | 0.99798 |
| 10 | 0.37513 | 2.24098 | 3.44E-04 | 0.1690 | 0.99967 |
| 11 | 0.5112 | 2.04002 | 1.69E-04 | 0.15824 | 0.99982 |

**Table S7**. Best fitted parameters ($\chi_T$, $\chi_S$, $\tau$ and $\alpha$) with the extended Debye model for complex **1** at 2 K in the H range 0-3000 Oe.

| H / Oe | $\chi_S$ / $cm^3mol^{-1}$ | $\chi_T$ / $cm^3mol^{-1}$ | $\tau$ / s | $\alpha$ | $R^2$ |
|---|---|---|---|---|---|
| 0 | 0.07962 | 11.35553 | 0.02678 | 0.2705 | 0.99979 |
| 200 | -0.01369 | 11.03342 | 0.03619 | 0.32551 | 0.99969 |
| 400 | -0.68729 | 13.26742 | 0.13297 | 0.49548 | 0.99965 |
| 600 | -0.02575 | 12.01932 | 0.22761 | 0.41078 | 0.99907 |
| 800 | 0.04069 | 11.57401 | 0.29179 | 0.38432 | 0.99965 |
| 1000 | 0.11196 | 11.19894 | 0.29220 | 0.38453 | 0.99982 |
| 1200 | 0.27158 | 10.86183 | 0.24012 | 0.40229 | 0.99988 |
| 1400 | 0.53596 | 11.03043 | 0.20322 | 0.45902 | 0.99983 |
| 1600 | 0.82108 | 11.3641 | 0.20231 | 0.53291 | 0.99972 |
| 1800 | 1.1579 | 10.32806 | 0.15154 | 0.53908 | 0.99993 |
| 2000 | 1.18684 | 9.6930 | 0.13851 | 0.54869 | 0.99993 |
| 2200 | 0.98042 | 9.3068 | 0.13960 | 0.5677 | 0.99987 |
| 2400 | 0.81932 | 8.72711 | 0.13339 | 0.56946 | 0.99992 |
| 2600 | 0.71529 | 8.00415 | 0.12191 | 0.55684 | 0.99983 |
| 2800 | 0.60279 | 7.60663 | 1.33E-01 | 0.55719 | 0.99985 |
| 3000 | 0.51075 | 7.22355 | 1.48E-01 | 0.55709 | 0.99983 |

**Table S8**. Best fitted parameters ($\chi_T$, $\chi_S$, $\tau$ and $\alpha$) with the extended Debye model for complex **1** at 800 Oe in the temperature range 2-10 K.

| T / K | $\chi_S$ / $cm^3mol^{-1}$ | $\chi_T$ / $cm^3mol^{-1}$ | $\tau$ / s | $\alpha$ | $R^2$ |
|---|---|---|---|---|---|
| 2 | 0.09362 | 12.44309 | 0.14673 | 0.39488 | 0.99998 |
| 2.2 | 0.09114 | 11.4835 | 0.12954 | 0.39474 | 0.99998 |
| 2.4 | 0.09157 | 10.42226 | 0.11065 | 0.39394 | 0.99989 |
| 2.6 | 0.08348 | 9.96637 | 0.10504 | 0.39936 | 0.99997 |

| | | | | | |
|---|---|---|---|---|---|
| 2.8 | 0.09441 | 9.06148 | 0.08717 | 0.39204 | 0.99996 |
| 3 | 0.10212 | 8.38759 | 0.07487 | 0.38687 | 0.9999 |
| 3.5 | 0.11309 | 7.14303 | 0.05353 | 0.38412 | 0.99987 |
| 4 | 0.13687 | 6.18953 | 0.03684 | 0.37323 | 0.99985 |
| 4.5 | 0.1615 | 5.48671 | 0.02505 | 0.36161 | 0.99985 |
| 5 | 0.1849 | 4.86712 | 0.01626 | 0.34852 | 0.99953 |
| 5.5 | 0.21276 | 4.39645 | 0.01063 | 0.33296 | 0.99951 |
| 6 | 0.23307 | 3.9973 | 0.00691 | 0.32253 | 0.99942 |
| 7 | 0.2897 | 3.37769 | 0.00292 | 0.30297 | 0.99932 |
| 8 | 0.36652 | 2.92882 | 0.00124 | 0.28995 | 0.9994 |
| 9 | 0.48556 | 2.5849 | 5.51E-04 | 0.27069 | 0.99962 |
| 10 | 0.64236 | 2.31729 | 2.76E-04 | 0.25048 | 0.99983 |

**Table S9**. Best fitted parameters ($\chi_T$, $\chi_S$, $\tau$ and $\alpha$) with the extended Debye model for compound **1$_{5\%}$** at 0 Oe in the temperature range 2-11 K.

| T / K | $\chi_S$ / $cm^3mol^{-1}$ | $\chi_T$ / $cm^3mol^{-1}$ | $\tau$ / s | $\alpha$ | $R^2$ |
|---|---|---|---|---|---|
| 2 | 4.60E-17 | 0.714 | 0.00103 | 0.52293 | 0.99944 |
| 2.2 | 1.20E-15 | 0.65543 | 9.95E-04 | 0.52098 | 0.99943 |
| 2.4 | 7.41E-16 | 0.59797 | 9.93E-04 | 0.52273 | 0.99958 |
| 2.6 | 4.27E-17 | 0.55234 | 9.97E-04 | 0.52114 | 0.99968 |
| 2.8 | 1.22E-15 | 0.51672 | 0.001 | 0.52457 | 0.99959 |
| 3 | 1.00E-15 | 0.48543 | 0.00103 | 0.52661 | 0.99946 |
| 3.25 | 1.00E-15 | 0.45324 | 0.00105 | 0.53013 | 0.99982 |
| 3.5 | 1.00E-16 | 0.42598 | 0.00107 | 0.53483 | 0.99975 |
| 3.75 | 2.88E-16 | 0.41001 | 0.00118 | 0.5463 | 0.99959 |
| 4 | 1.83E-16 | 0.38465 | 0.00113 | 0.54101 | 0.99941 |
| 4.25 | 3.37E-17 | 0.37023 | 0.00124 | 0.539 | 0.99958 |
| 4.5 | 1.00E-15 | 0.35245 | 0.00117 | 0.53749 | 0.99962 |
| 4.75 | 0.01008 | 0.33315 | 0.0013 | 0.51022 | 0.99899 |
| 5 | 0.01636 | 0.31724 | 0.00135 | 0.49896 | 0.99916 |
| 5.5 | 0.02283 | 0.28683 | 0.00132 | 0.45158 | 0.99868 |
| 6 | 0.01575 | 0.26982 | 0.00116 | 0.45717 | 0.99883 |
| 6.5 | 0.02149 | 0.24569 | 9.56E-04 | 0.40327 | 0.99845 |
| 7 | 0.04421 | 0.21915 | 8.93E-04 | 0.34835 | 0.9992 |
| 8 | 0.03775 | 0.19117 | 5.13E-04 | 0.30437 | 0.9992 |
| 9 | 0.0465 | 0.17153 | 3.35E-04 | 0.22194 | 0.99648 |
| 10 | 0.0485 | 0.1516 | 1.72E-04 | 0.17 | 0.9995 |
| 11 | 0.06481 | 0.1381 | 1.22E-04 | 0.08646 | 0.99902 |

**Table S10**. Best fitted parameters ($\chi_T$, $\chi_S$, $\tau$ and $\alpha$) with the extended Debye model for compound $\mathbf{1_{5\%}}$ at 800 Oe in the temperature range 3-12 K.

| T / K | $\chi_S$ / $cm^3mol^{-1}$ | $\chi_T$ / $cm^3mol^{-1}$ | $\tau$ / s | $\alpha$ | $R^2$ |
|---|---|---|---|---|---|
| 3 | 5.91E-03 | 0.61089 | 2.71983 | 0.29016 | 0.99931 |
| 3.25 | 6.28E-03 | 0.51292 | 1.27E+00 | 0.24623 | 0.99914 |
| 3.5 | 6.96E-03 | 0.45714 | 6.92E-01 | 0.21489 | 0.99958 |
| 3.75 | 6.37E-03 | 0.41764 | 4.06E-01 | 0.19292 | 0.99951 |
| 4 | 6.40E-03 | 0.38735 | 0.25404 | 0.18327 | 0.99971 |
| 4.25 | 5.70E-03 | 0.36183 | 0.16349 | 0.17395 | 0.9997 |
| 4.5 | 5.66E-03 | 0.34211 | 0.11072 | 0.16992 | 0.99961 |
| 4.75 | 5.70E-03 | 0.32128 | 0.07596 | 0.16016 | 0.99956 |
| 5 | 5.69E-03 | 0.30515 | 0.05386 | 0.15659 | 0.99954 |
| 5.5 | 5.93E-03 | 0.27723 | 0.02905 | 0.15244 | 0.99936 |
| 6 | 5.31E-03 | 0.25315 | 0.01665 | 0.15084 | 0.99951 |
| 6.5 | 4.15E-03 | 0.23715 | 0.01033 | 0.16166 | 0.99911 |
| 7 | 0.00847 | 0.21844 | 0.00637 | 0.15289 | 0.99907 |
| 8 | 0.00959 | 0.19584 | 0.00258 | 0.1969 | 0.99888 |
| 9 | 0.02046 | 0.16914 | 0.00109 | 0.17402 | 0.99883 |
| 10 | 0.03091 | 0.15266 | 5.15E-04 | 0.16948 | 0.99929 |
| 11 | 0.04655 | 0.13832 | 2.93E-04 | 0.10948 | 0.99969 |
| 12 | 0.05868 | 0.12607 | 1.66E-04 | 0.04686 | 0.99967 |

**Table S11**. The Basis set used in *ab initio* calculations for complex **1** and **2**, model structure **1'** and model **1''**.

| Atoms | Basis Set |
|---|---|
| Dy | ANO-RCC…8s7p4d3f2g1h. |
| Tb | ANO-RCC…8s7p4d3f2g1h. |
| Lu | ANO-RCC…8s7p4d3f2g1h. |
| C | ANO-RCC…3s2p. |
| O | ANO-RCC...4s3p2d. |
| N | ANO-RCC...4s3p2d. |
| H | ANO-RCC…2s |

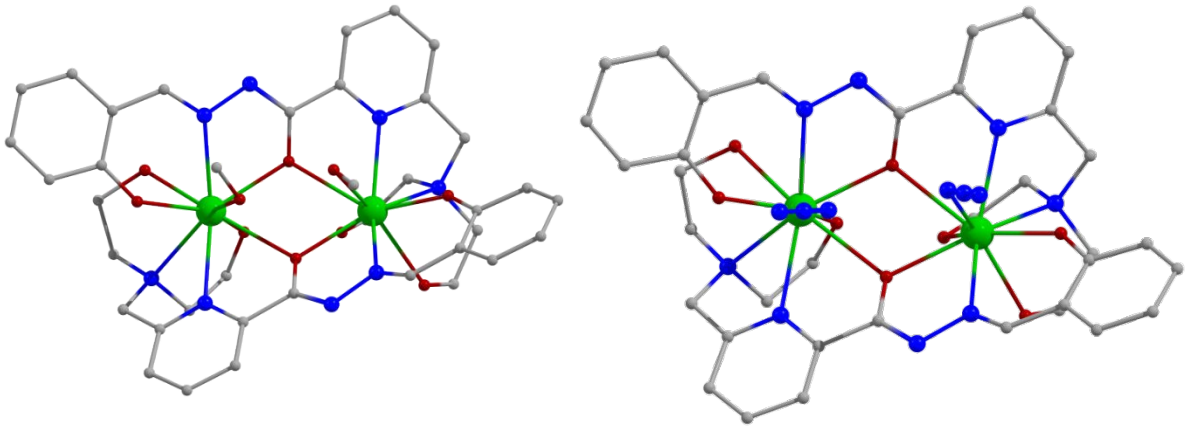

**Figure S25**: Model structure for **1'** and **1''**.

**Table S12**: Energy distribution in low lying 8 KDs for complexes **1**, model **1'** and model **1''**.

| KD | Energy of the Complexes | | | | | |
|---|---|---|---|---|---|---|
| | **1 Dy-1** | **1 Dy-2** | **1a Dy-1** | **1a Dy-2** | **1b Dy-1** | **1b Dy-2** |
| 1 | 0.00 | 0.00 | 0.00 | 0.00 | 0.00 | 0.00 |
| 2 | 176.34 | 117.65 | 185.38 | 137.47 | 178.54 | 131.48 |
| 3 | 339.55 | 200.53 | 363.93 | 202.30 | 344.86 | 208.11 |
| 4 | 449.23 | 256.10 | 478.51 | 289.06 | 424.59 | 290.41 |
| 5 | 519.12 | 331.06 | 551.76 | 377.97 | 513.13 | 381.58 |
| 6 | 584.40 | 383.67 | 614.30 | 441.44 | 593.67 | 470.17 |
| 7 | 709.89 | 434.20 | 728.44 | 525.36 | 710.24 | 566.83 |
| 8 | 820.83 | 536.04 | 829.80 | 630.91 | 823.47 | 674.98 |

**Table S13**: Energy distribution in low lying 13 *Ising* doublets for complexes **2**.

| KD | Energy(Tb1) | Energy (Tb2) |
|---|---|---|
| 1 | 0.00 | 0.00 |
| 2 | 0.19 | 0.15 |
| 3 | 142.22 | 101.21 |
| 4 | 145.10 | 104.56 |
| 5 | 261.20 | 181.63 |
| 6 | 282.62 | 204.65 |
| 7 | 361.29 | 256.92 |
| 8 | 430.80 | 319.70 |
| 9 | 470.07 | 346.98 |
| 10 | 576.45 | 416.09 |
| 11 | 588.90 | 427.59 |
| 12 | 788.15 | 536.91 |
| 13 | 789.57 | 538.78 |

**Table S14**: Crystal field parameters for complex **1**, model 1', model 1'' and complex **2**.

| K | q | A(k,q) | | | | | | | |
|---|---|---|---|---|---|---|---|---|---|
| | | 1-Dy1 | 1-Dy2 | 1a-Dy1 | 1a-Dy2 | 1b-Dy1 | 1b-Dy2 | 2-Tb1 | 2-Tb2 |
| 2 | -2 | -3.59E+00 | 1.60E+00 | -8.75E-01 | 6.87E-01 | -7.90E-01 | -1.43E-01 | 1.12E+00 | -1.60E+01 |
| 2 | -1 | -5.30E-01 | 8.77E-01 | -1.76E-01 | 3.31E-02 | -2.05E-02 | -4.23E-01 | 4.19E+00 | -1.31E+01 |
| **2** | **0** | **-8.98E+00** | **-2.35E+00** | **-4.01E+00** | **-2.71E+00** | **-3.80E+00** | **-2.94E+00** | **-2.61E+01** | **-1.58E+01** |
| 2 | 1 | 3.67E+00 | 4.52E-01 | 2.03E+00 | -1.55E+00 | 2.59E+00 | -1.39E+00 | 3.06E+01 | -2.60E+01 |
| 2 | 2 | 5.82E+00 | 1.07E+00 | 2.31E+00 | 2.89E+00 | 2.79E+00 | 3.37E+00 | 1.88E+01 | -6.78E+00 |
| | | | | | | | | | |
| 4 | -4 | -3.91E-02 | -5.84E-04 | -6.73E-03 | 5.03E-03 | -3.79E-03 | 4.65E-03 | -7.56E-01 | -7.84E-01 |
| 4 | -3 | -2.19E-01 | 3.21E-02 | -3.09E-02 | -3.54E-02 | -2.73E-02 | -4.08E-02 | 2.85E+00 | -8.25E-01 |
| 4 | -2 | -8.83E-02 | 3.18E-03 | -1.26E-02 | 4.19E-03 | -9.46E-03 | 5.09E-03 | -3.96E-01 | 1.73E-01 |
| 4 | -1 | 4.81E-02 | -1.59E-03 | 6.08E-03 | -3.40E-03 | 4.36E-03 | -5.52E-04 | -9.93E-01 | -1.01E-01 |
| 4 | 0 | -2.67E-02 | -1.92E-03 | -4.02E-03 | -2.00E-03 | -4.17E-03 | -1.63E-03 | 9.02E-02 | 6.40E-02 |
| 4 | 1 | -8.18E-02 | -4.27E-03 | -1.24E-02 | 1.17E-02 | -1.84E-02 | 1.03E-02 | -1.91E+00 | 6.09E-01 |
| 4 | 2 | -1.36E-02 | -2.43E-03 | -8.86E-04 | -1.03E-03 | -3.73E-03 | -2.48E-03 | 3.85E-01 | 9.41E-02 |
| 4 | 3 | -5.33E-02 | -2.60E-02 | -3.09E-03 | 7.92E-03 | -6.44E-03 | -1.75E-03 | 8.54E-01 | 3.62E+00 |
| 4 | 4 | -3.16E-02 | -1.10E-02 | -4.13E-03 | -7.25E-03 | -7.39E-03 | -7.70E-03 | -2.80E-01 | 4.84E-02 |
| | | | | | | | | | |
| 6 | -6 | 1.07E-02 | 2.39E-04 | 4.04E-04 | 8.34E-05 | 4.05E-04 | 2.18E-05 | -1.67E-01 | -7.40E-02 |
| 6 | -5 | -2.32E-02 | -1.32E-03 | -1.08E-03 | 1.14E-03 | -9.56E-04 | 9.32E-04 | -7.88E-02 | 1.13E+00 |
| 6 | -4 | 2.98E-03 | 9.93E-05 | 1.15E-04 | 1.21E-04 | 1.53E-04 | 7.00E-05 | 9.88E-02 | -2.15E-01 |
| 6 | -3 | 2.30E-03 | -5.14E-04 | 1.12E-04 | 5.68E-04 | 7.32E-05 | 4.68E-04 | -2.64E-01 | 2.02E-01 |
| 6 | -2 | 3.48E-03 | 3.82E-05 | 1.49E-04 | 4.15E-05 | 1.41E-04 | 3.74E-05 | -4.26E-02 | -1.42E-01 |
| 6 | -1 | -2.29E-03 | -9.30E-05 | -9.49E-05 | 1.05E-04 | -8.13E-05 | 9.73E-05 | 1.58E-01 | -5.67E-02 |
| 6 | 0 | 4.75E-04 | 6.26E-06 | 2.42E-05 | 3.20E-06 | 2.47E-05 | 6.02E-06 | -8.32E-03 | 1.18E-02 |
| 6 | 1 | -4.30E-04 | -4.23E-05 | -1.48E-05 | 3.60E-05 | 2.99E-05 | 2.41E-05 | 1.98E-01 | -1.53E-01 |
| 6 | 2 | 6.15E-04 | 3.53E-05 | 9.44E-06 | 1.46E-05 | 2.58E-05 | 5.16E-05 | 3.86E-02 | 2.01E-01 |
| 6 | 3 | 4.59E-03 | 3.97E-05 | 1.50E-04 | 8.15E-05 | 1.20E-04 | 2.11E-04 | 2.49E-01 | -3.43E-01 |
| 6 | 4 | -1.54E-03 | 3.92E-05 | -8.33E-05 | 3.44E-05 | 6.47E-05 | 9.72E-05 | 2.15E-01 | -7.20E-02 |
| 6 | 5 | -2.58E-03 | 1.32E-04 | -4.33E-05 | 5.03E-04 | -8.95E-04 | 9.58E-04 | 1.09E+00 | -3.97E-01 |
| 6 | 6 | -3.94E-03 | 2.44E-05 | -2.70E-04 | 8.06E-05 | 6.62E-05 | 1.52E-04 | -8.02E-01 | -6.77E-02 |

The crystal field parameters are calculated using the following Hamiltonian,

$H_{CF} = \sum_{k,q} B_k^q O_k^q$…….(Equation 1)

Where $O_k^q = extended\ stevens\ operator$

k=rank of ITO=2,4,6

q=component of the ITO = -k,-k+1,….,0,….,k.

Following Hamiltonian below is used for calculating the dipolar and exchange interaction between the $Ln^{III}$-$Ln^{III}$ centres.

$$\hat{H}_{ex} = -\sum_i J_i S_i S_{i+1} \quad \text{(Equation 2)}$$

Here $J_i = J_{idip} + J_{iexch}$; that is, $J_i$ are the total magnetic interaction Ln-Ln, this describes the interaction between the neighbouring metal centres.

$$\hat{H} = -(-J_{dip}^{Ln^i - Ln^{i+1}} + J_{exch}^{Ln^i - Ln^{i+1}})\tilde{s}_{Ln_i}\tilde{s}_{Ln_{i+1}} \quad \text{(Equation 3)}$$

$$J_{dip}^{Ln^i - Ln^{i+1}} = \frac{\mu_B^2}{R^3_{Dy^i - Dy^{i+1}}} g_{Ln}^2 \quad \text{(Equation 4)}$$

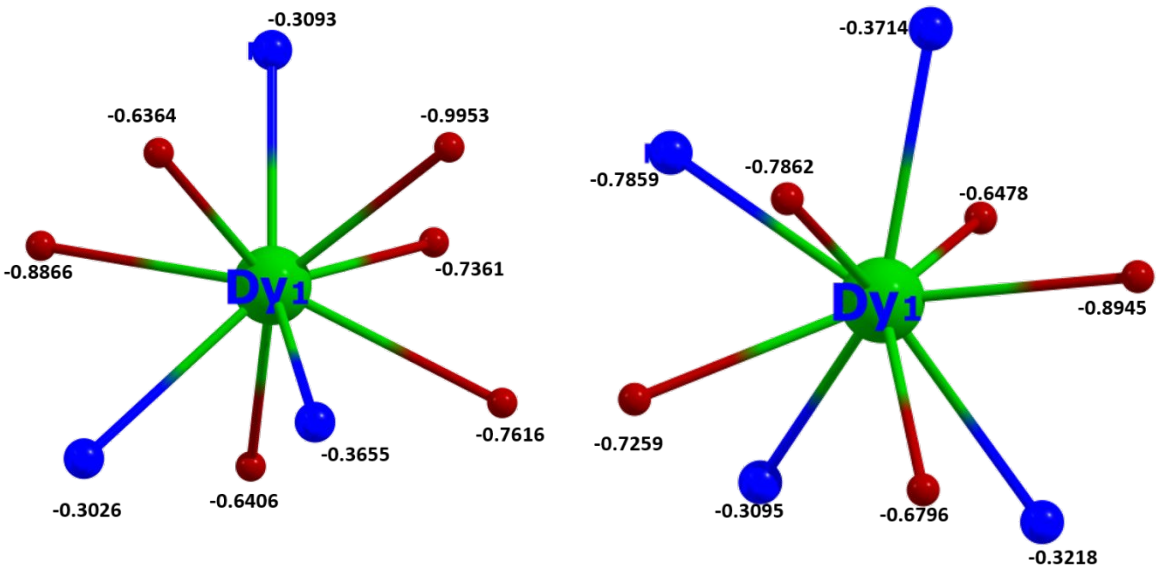


**Figure S26**: Loprop charge distribution for complex **1**.

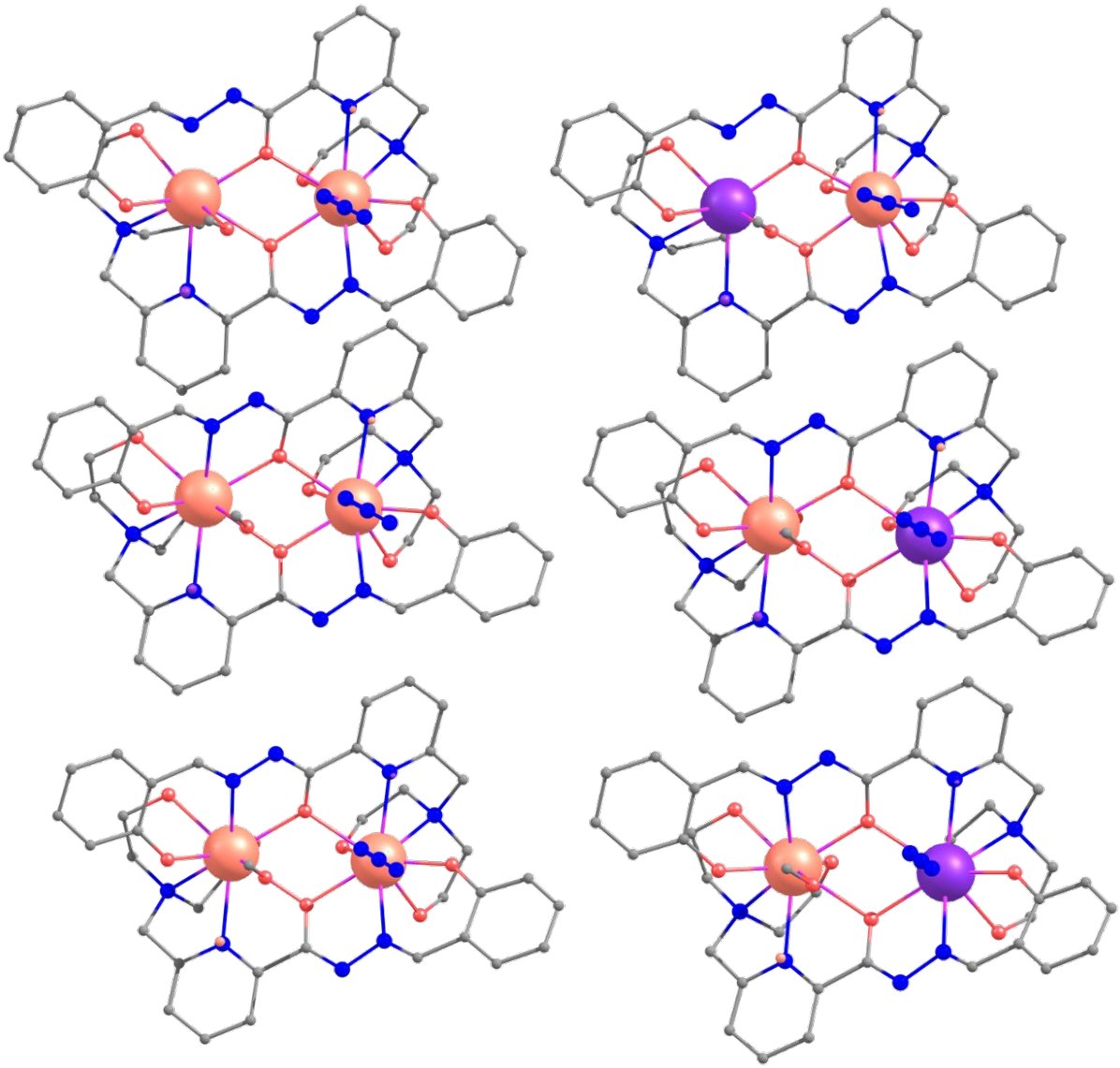

**Figure S27**: DFT computed spin density on Ln centre using Broken symmetry approach for complex **1-3**.

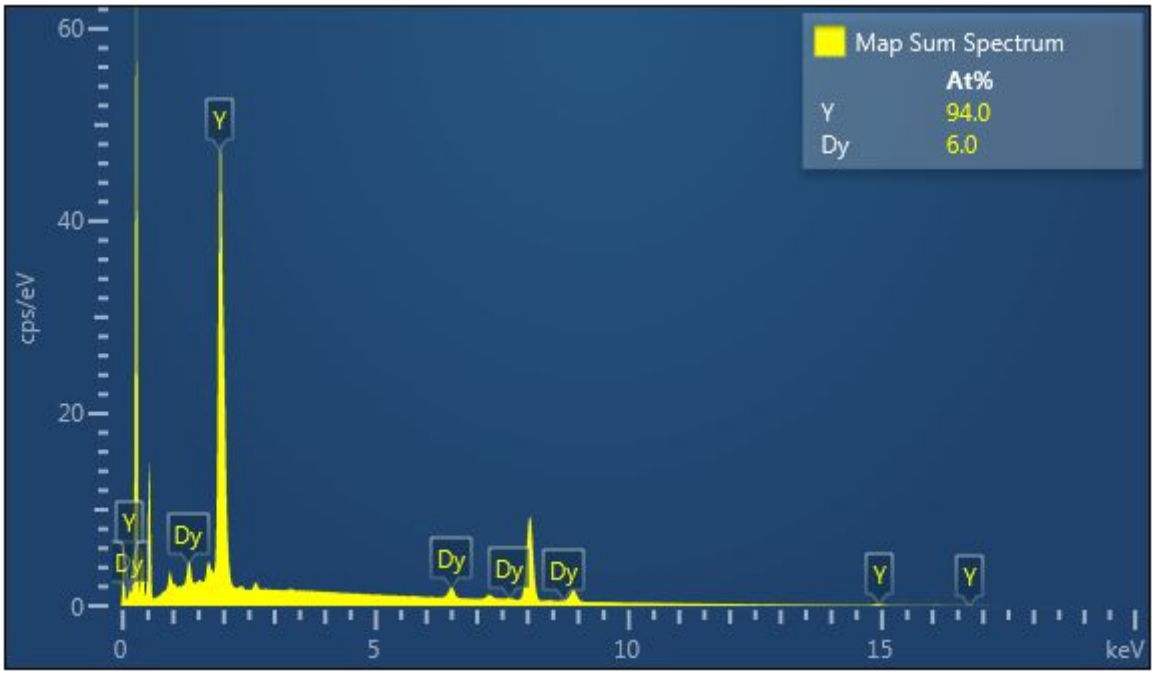


**Figure S28**: EDS spectrum for complex $\mathbf{1}_{5\%}$. The spectrum was analysed by FESEM model JSM 7200F with FEG source.